Measurement of ultralow radiation-induced charge densities using picosecond mid-IR laser-induced breakdown: supplementary material

DANIEL WOODBURY, ROBERT M. SCHWARTZ, AND HOWARD M. MILCHBERG[*]

Institute for Research in Electronics and Applied Physics, University of Maryland, College Park, Maryland 20742, USA
Corresponding author: milch@umd.edu

This document provides supplementary information to "Measurement of ultralow radiation-induced charge densities using picosecond mid-IR laser-induced breakdown," https://doi.org/10.1364/OPTICA.6.000811. Provided are details on (I) radiation-induced ion formation in air, (II) wavelength-time mapping of the pump pulse and analysis of collected spectra, (III) the plasma density detection threshold, (IV) discussion of background signals, and (V) a more detailed description of the 0D avalanche model.

I. Ion formation and evolution

The 5.3 MeV α-particles from the Po-210 source deposit energy through inelastic collisions with neutral molecules, generating local ionization exceeding that caused by naturally occurring sources of radiation. Within tens of nanoseconds, the radiation-generated free electrons attach to neutral oxygen molecules to form O_2^- [1,2]. The O_2^- ions form the beginning of a chain of air chemistry reactions, resulting in more tightly bound ions such as NO_2^-, O_3^-, O^- and OH^- and the terminal ion NO_3^- [3,4]. At background levels of radioactivity (ionization rate ~30 $cm^{-3}s^{-1}$), a simple rate equation model [1] that considers only O_2^- ions (and neglects subsequent air chemistry) gives a free electron density ~10^{-2} cm^{-3} and O_2^- density ~10^4 cm^{-3}. Within an α-particle stopping distance (< 3 cm) from our 5 mCi α-source, (ionization rate roughly ~7×10^{10} $cm^{-3}s^{-1}$), the model predicts electron and O_2^- seed densities of ~10^2 cm^{-3} and ~10^8 cm^{-3}. Since this model ignores subsequent air chemistry, it overestimates the O_2^- density, but it should give a reasonable estimate of the total negative ion density.

II. Time-wavelength mapping of spectra

Mid-IR laser pulses at λ=3.9 (3.6-4.2) µm are generated through optical parametric amplification of a chirped λ=1.45 (1-4-1.5) µm signal beam with a narrowband λ=1.064 µm pump [5]. Wavelength-to-time mapping is established by performing a cross correlation measurement between a λ=1024 nm (274 fs FWHM duration) reference beam and the stretched 1.45 µm signal beam. At each time delay, the peak wavelength of the sum frequency signal is recorded, with results shown in Fig. S1. This measurement

also gives the time-to-wavelength mapping of the mid-IR pump beam as determined by calculating the wavelength mixing in cross correlation and amplification, as shown on the right scale in Fig. S1. The chirp is nearly linear, an approximation we will use in our time resolution and threshold estimates below.
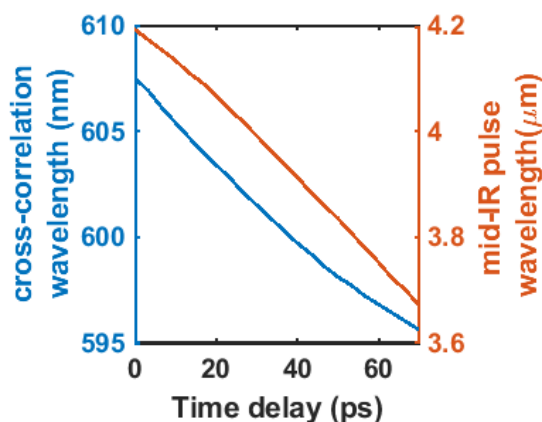
Fig. S1. Results of cross correlation measurement of the 1.45 µm signal beam with a 1024 nm reference beam (left scale), and the calculated time dependence of the mid-IR pump spectrum (right scale).

Reference spectra were collected on a mid-IR spectrometer which spread out the whole pump spectrum (3.65-4.2 µm, 70 ps) over ~350 pixels on the spectrometer, which gives a temporal resolution of τ_{pixel}~0.2 ps. The spectrometer was calibrated by using higher-order diffraction of a 532 nm laser diode. In order to

improve extraction of breakdown onset times, spectra were smoothed with a 10 point moving average (reducing temporal resolution to ~2 ps). The longest wavelength (and correspondingly, earliest point in time) where the backscattered spectrum exceeds the detector noise threshold of ~2 counts is defined as the breakdown time. Time advance is then determined by comparing the breakdown time to the end of the pulse, which we define as the point when the pump intensity drops to 10% of its peak value (λ=3.65 µm).

III. Breakdown detection threshold

The electron density corresponding to the breakdown detection threshold is estimated by assuming Fresnel reflection from a sharp plasma density step. For a sharp boundary, the total reflection is given by $R = \left|\frac{n_1-n_2}{n_1+n_2}\right|^2$, where n_1 and n_2 are the indices of refraction on either side of the interface. For a plasma well below the critical density, $N_{cr} = \frac{1.1\times10^{21}}{\lambda[\mu m]^2}\,\text{cm}^{-3} = 7.2\times10^{19}\,\text{cm}^{-3}$ at $\lambda = 3.9\mu m$, the plasma index of refraction is $n_2 \cong 1 - \frac{N_e}{2N_{cr}}$, such that $R = \left|\frac{N_e/2N_{cr}}{2}\right|^2 = \frac{N_e^2}{16N_{cr}^2}$ for $n_1 = 1$. The size of the plasma before saturation and late-time heating is limited by electrostatic plasma forces to a sphere of approximate radius $r\sim 5\,\mu m$, as discussed in the main text, so the fractional beam energy backscattered by a single breakdown site (at threshold) is $\frac{\pi r^2}{\pi w_0^2}$, where w_0=120µm is the beam spot size.

Assuming that the backscattered energy is spread over 2π radians, the collection efficiency is $\eta = \frac{1}{2(f/\#)^2}$ ~8×10^{-5} for f/80 collection optics. The collected energy is spread out spectrally on the InSb detector, and the FWHM length of the pulse, $\tau_{pulse}\sim 50$ ps , dictates that the energy backscattered and collected on a single pixel for incident laser energy E_0 is

$$E_{pixel} = E_0 \left(\frac{N_e^2}{16N_{cr}^2}\right)\frac{r^2}{w_0^2}\,\eta\,\frac{\tau_{pixel}}{\tau_{pulse}}. \qquad (S1)$$

To detect this backscattered energy, the energy/pixel must be above the background noise. The detector showed a noise threshold of $NT\sim 2$ counts, with each count corresponding to $q\sim 400$ electrons. The quantum efficiency QE of the camera in the spectral range of the pump is 90%, and the photon energy needed to generate one electron is $h\nu = 0.31$ eV. So the energy/pixel needed for detection just above the noise threshold is

$$E_{pixel,thresh} = NT \times \frac{q}{QE}h\nu. \qquad (S2)$$

Setting $E_{pixel} > E_{pixel,thresh}$ for a typical incident energy E_0=20 mJ, gives a threshold detectable plasma density of

$$N_{e,thresh} = 4\,N_{cr}\sqrt{NT \times \frac{q}{QE}\frac{h\nu}{\eta}\frac{1}{E_0}\frac{w_0^2}{r^2}\frac{\tau_{pulse}}{\tau_{pixel}}}$$
$$= 6\times10^{17}\,cm^{-3}.$$
$$(S3)$$

An important scaling from Eq. (S3) is $N_{e,thresh} \propto f/\#$. Assuming backscatter collection with the same optic used to focus the laser, the scaling at range requires an avalanche driven closer to saturation.

IV. Background counts

The appearance of bright breakdowns, which resulted in high values of plasma emission, mid-IR backscatter, and large time advances well above those observed for single electron seeds, suggest interaction with higher density material with a much higher avalanche growth rate. These background counts were also observed independent of distance from the radioactive source, suggesting an environmental source. This is consistent with seeding by aerosols (such as dust particles or small liquid droplets) in laboratory air, since the locally high material density in airborne particulates increases the collisional rate, greatly speeding up breakdown and lowering the threshold for achieving it. Prior experiments have observed avalanche thresholds reduced by one to two orders of magnitude in "dirty" air compared to filtered laboratory air [6]. The frequency of these breakdowns (2-3% of all shots) extended across all pump intensities, consistent with a greatly reduced breakdown threshold depending far less on the peak intensity than on whether a dust particle is somewhere in the focal volume.

V. Description of 0D Model

The 0D model calculates single- and multi-photon ionization, collisional ionization, electron attachment, electron-ion dissociative recombination, and collisional negative ion detachment as a function of the plasma temperature, density, and laser pulse intensity [1]. The version used here includes collisional ionization rates, and molecular dissociation and ionization loss rates appropriate at the higher temperatures achieved in picosecond breakdowns [7,8]. The electron density and temperature calculated by the model follow the 70 ps pump intensity envelope nearly adiabatically: In response to step changes in intensity, runs with the 0D model predict fast equilibration (~2 ps) to a new quasi-steady state temperature and density. We therefore extract intensity-dependent temperatures and growth rates from the 0D simulation and use these parameters to grow the number of electrons over the 70 ps (50 ps FWHM) duration of the laser pulse.

References

1. J. Isaacs, C. Miao, and P. Sprangle, "Remote monostatic detection of radioactive material by laser-induced breakdown," Phys. Plasmas **23,** 033507 (2016).
2. M. L. Huertas, J. Fontan, and J. Gonzalez, "Evolution times of tropospheric negative ions," Atmos. Environ. **12,** 2351-2362 (1967).
3. V. A. Mohnen, "Discussion of the formation of major positive and negative ions up to the 50 km level," Pure Appl. Geophys. **84,** 141–151 (1971).
4. M. L. Huertas, J. Fontan, "Formation of stable positive and negative small ions of tropospheric interest," Atmos. Environ. **16,** 2521–2527 (1982).
5. G. Andriukaitis, T. Balčiūnas, S. Ališauskas, A. Pugžlys, A. Baltuška, T. Popmintchev, M.-C. Chen, M. M. Murnane, and H. C. Kapteyn, "90 GW peak power few-cycle mid-infrared pulses from an optical parametric amplifier," Opt. Lett. **36**, 2755 (2011).
6. C. G. Morgan, "Laser-induced breakdown of gases," Rep. Prog. Phys. **38**, 621-665 (1975).
7. A. W. Ali, "Electron Energy Loss Rates in N2, O2, and Air," NRL Memorandum Report 5400 (1984).
8. J. Isaacs, D. Woodbury, P. Sprangle, "Remote detection of radioactive material using optically induced air breakdown ionization," submitted to Proc. SPIE, 11010-50.